An accurate spectral/discontinuous finite-element formulation of a phase-space-based level set approach to geometrical optics

Bernardo Cockburn [a], Jianliang Qian [b],
Fernando Reitich [a,*] and Jing Wang [c]

[a] *School of Mathematics, University of Minnesota, Minneapolis, MN 55455*
[b] *Department of Mathematics, University of California, Los Angeles, CA 90095*
[c] *Institute for Mathematics and its Applications, Minneapolis, MN 55455*

Abstract

In this paper we introduce a new numerical procedure for simulations in geometrical optics that, based on the recent development of Eulerian phase-space formulations of the model, can deliver very accurate, uniformly resolved solutions which can be made to converge with arbitrarily high orders in general geometrical configurations. Following previous treatments, the scheme is based on the evolution of a wavefront in phase-space, defined as the intersection of level sets satisfying the relevant Liouville equation. In contrast with previous work, however, our numerical approximation is specifically designed (i) to take full advantage of the smoothness of solutions, and (ii) to facilitate the treatment of scattering obstacles, all while retaining high-order convergence characteristics. Indeed, to incorporate the full regularity of solutions that results from the unfolding of singularities, our method is based on their *spectral* representation; to enable a simple high-order treatment of scattering boundaries, on the other hand, we resort to a *discontinuous Galerkin* finite element method for the solution of the resulting system of equations. The procedure is complemented with the use of a recently derived SSP-RK scheme for the time integration that, as we demonstrate, allows for overall approximations that are rapidly convergent.

Key words: wave equation, eikonal equation, Liouville equation, geometrical optics, spectral methods, discontinuous Galerkin

* Corresponding author.
  Email addresses: `cockburn@math.umn.edu` (Bernardo Cockburn), `qian@math.ucla.edu` (Jianliang Qian), `reitich@math.umn.edu` (Fernando Reitich), `jwang@ima.umn.edu` (Jing Wang).

1 Introduction

The recognition that numerical simulation of scattering processes can greatly accelerate the assessment and design of new technology has translated into its integration in the most varied engineering applications that rely on wave phenomena. Indeed, today numerical simulations of wave propagation guide developments in areas ranging from radar, sonar and remote sensing to electronics and microscopy. As a result, and due to the increasing demands for accuracy and speed, the need for improved numerical algorithms for the treatment of such problems continues to intensify, as algorithmic advances can immediately enable corresponding technological gains. Over the last two decades, a variety of advanced numerical methods have been developed to accurately and efficiently solve full-wave models of electromagnetic, acoustic and elastic wave propagation; see e.g. [3,5,9,20,28,35] and the references cited there. By the very nature of these models, however, rigorous methods for their numerical solution are limited in the range of frequencies they can practically deal with, as their accuracy hinges on the full resolution of the wavelength of oscillation of field quantities. As a consequence, relevant simulations in a variety of applications, such as in seismic exploration [12] or in high-frequency radar [6], are beyond the reach of full-wave solvers and must, instead, be based on approximate models. Among these, perhaps the simplest and most broadly used is the "geometrical optics" (GO) model that results as a lowest order (WKB) approximation of wave-like equations as the frequency becomes infinite [36]. In this paper we introduce a new numerical procedure for simulations in geometrical optics that, based on the recent development of Eulerian phase-space formulations of the model [17,23], can deliver very accurate, uniformly resolved solutions which can be made to converge with arbitrarily high orders in general geometrical configurations.

The need for improved GO solvers can perhaps be most easily explained by noting that the current state-of-the-art in a number of complex applications relies on, albeit quite sophisticated, "ray-tracing"; see e.g. [2]. As has been recognized [16], however, the Lagrangian nature of ray-tracing can present difficulties (e.g. divergent rays leading to uneven resolution) which have prompted the recent development of new computational methods based on (Eulerian) solution of partial differential equations. Early versions of this approach concentrated on the design of upwind [33,34] and ENO schemes [18] for the direct solution of the eikonal equation, leading to accurate approximations of the viscosity solution [15]. This (single-valued) solution, however, represents only the wave of first arrival at any given point [15] which may be insufficient for certain applications. Indeed, for instance, in seismics waves with larger travel-times may carry significantly more energy than that of the viscosity solution [22], while accounting for multiple reflections in electromagnetics may be essential in constructing accurate approximations for wave fields [8]. For this reason, a

2

number of algorithms have been recently developed to upgrade the viscosity solution to the multi-valued solution relevant in these cases. Among these we encounter, for instance, the "big ray tracing method" [1], the "method of decomposition along caustics" [4] and the "slowness matching method" [31,32]. All of these procedures are based on domain decomposition and local approximations of viscosity solutions, which are then combined into a multi-valued quantity.

An alternative approach to the approximation of multi-valued solutions is based on a "kinetic" formulation that views rays as trajectories of particles following a Hamiltonian dynamics; see [16] and the references therein. In this approach, multi-valued solutions are naturally "unfolded" through the introduction of conjugate phase variables. This, however, is achieved at the expense of doubling the number of independent variables, with the consequent potential for increased computational cost. To deal with this problem, two alternative strategies have been developed, leading to "wavefront" and "moment-based" methods respectively [16]. In the former, an interface representing a wavefront is evolved following the Liouville formulation, while the latter is based on the derivation of new equations (for the moments of the density) with fewer unknowns. Here we propose a new approximation scheme based on the kinetic viewpoint that can be interpreted as combining elements from these two approaches. Indeed, as we further explain below, as in wavefront methods our strategy is based on the evolution of an interface which, following [23], we define as the intersection of level sets of functions satisfying the Liouville equations. In contrast with [23], however, we do not resort to direct discretization of the phase variables. Rather, the procedure we present below relies on suitable (spectral) representations of the densities, and on the solution of the resulting equations for the coefficients in these expansions. In this sense then, our approach can be related to moment-based methods where our "moments" are not necessarily chosen to be integrals against monomials in phase variables needing a "closure hypothesis", but rather against basis functions that guarantee accurate representations of general phase variations.

Our work is largely motivated by the developments in [23] (see also [11,25,26]). Indeed, as we mentioned, we shall follow this work and seek to approximate solutions to Liouville equations that implicitly define the wavefront. In [23] the approximation procedure relied on spatial finite differences and Runge-Kutta time discretizations. More precisely, away from scattering boundaries, a fifth-order WENO-Godunov [21] scheme was used for the space and phase variables while a third-order TVD-RK procedure [27] (or a fourth order SSP-RK method [29]) was implemented to march forward in time; when dealing with (reflecting) boundaries [11], on the other hand, the order of the spatial discretization was reduced to first, due to the complications that arise in attempting to devise higher-order differencing schemes in such situations. Our approach, on the other hand, is based on entirely different discretizations

which are designed (i) to take full advantage of the smoothness of solutions to the Liouville equations, and (ii) to facilitate the treatment of scattering obstacles, all while retaining high-order convergence characteristics. Indeed, as we further detail below, to incorporate the full regularity of solutions that results from the unfolding of singularities our method is based on their *spectral* representation; to enable a simple high-order treatment of scattering boundaries, on the other hand, we resort to a *discontinuous Galerkin* [13,14] finite element method (DGFEM) for the solution of the resulting system of equations. For the time integration, finally, the procedure is complemented with the use of a recently derived SSP-RK scheme [10,19] which, as we demonstrate below, allows for overall approximations that are rapidly convergent.

The rest of the paper is organized as follows. First, in §2 we briefly review the relevant equations and, in particular, we introduce the phase-space (Liouville) formulation of the GO problem. Then, in §3 we introduce and analyze the spectral/DGFEM approximation. In particular, in §3.1 we demonstrate that the resulting (hyperbolic) system for the spectral coefficients can be *explicitly* diagonalized. This, in turn, allows for an explicit implementation of an "up-winded" DGFEM, as we describe in §3.2. The integration of (reflecting and absorbing) boundary conditions within our new formulation is then detailed in §4 and followed, in §5, by some numerical results in two space dimensions (three-dimensional reduced phase-space). Finally, some comments on extensions (e.g. to physical three-dimensional space) and possible improvements (e.g. relating to high-order localization) are collected in §6.

2 Phase-space-based geometrical optics

The basic model for high-frequency wave propagation is provided by the *eikonal equation* [7,36]

$$S_t(\mathbf{x}, t) + c(\mathbf{x})|\nabla_{\mathbf{x}} S(\mathbf{x}, t)| = 0, \quad \mathbf{x} \in \mathbb{R}^d \ (d = 2, 3), \tag{1}$$

for the phase S of the (acoustic/electromagnetic) field, where $c(\mathbf{x})$ denotes the local wave velocity. As we mentioned, adding to the challenges stemming from its nonlinear character, the difficulties associated with the solution of (1) are compounded in situations where its multi-valued solutions are of interest. In this case, as we explained above, an alternative to Lagrangian ray-tracing is provided by a formulation that views rays as trajectories of particles following the Hamiltonian dynamics

$$\begin{cases} \frac{d\mathbf{x}}{dt} = \nabla_{\mathbf{p}} H(\mathbf{x}, \mathbf{p}) = c(\mathbf{x})\frac{\mathbf{p}}{|\mathbf{p}|} \\ \frac{d\mathbf{p}}{dt} = -\nabla_{\mathbf{x}} H(\mathbf{x}, \mathbf{p}) = -|\mathbf{p}|\nabla_{\mathbf{x}} c(\mathbf{x}) \end{cases} \tag{2}$$

in the phase-space $(\mathbf{x}, \mathbf{p})$, where $H(\mathbf{x}, \mathbf{p}) = c(\mathbf{x})|\mathbf{p}|$. With this interpretation, a "particle density function" $f(\mathbf{x}, \mathbf{p}, t)$ will satisfy the *Liouville equation* [16]

$$f_t(\mathbf{x}, \mathbf{p}, t) - \nabla_{\mathbf{p}} f \cdot |\mathbf{p}|\nabla_{\mathbf{x}}c + \nabla_{\mathbf{x}}f \cdot c(\mathbf{x})\frac{\mathbf{p}}{|\mathbf{p}|} = 0. \tag{3}$$

This equation displays the same characteristic strips as the original eikonal equation (1) but the introduction of phase variables $(\mathbf{p})$ "unfolds" multi-valued solutions. Moreover, this equation can be further simplified by appealing to the condition that the Hamiltonian remain constant along characteristics. Indeed, the normalization $H \equiv 1$, for instance, leads to the constraint

$$|\mathbf{p}| = \frac{1}{c(\mathbf{x})}$$

which can be used to restrict the solutions of (3) to those of the form

$$f(\mathbf{x}, \mathbf{p}, t) = c(\mathbf{x})\delta\left(|\mathbf{p}| - c(\mathbf{x})^{-1}\right) u(\mathbf{x}, \mathbf{p}/|\mathbf{p}|, t).$$

For example, in two space dimensions, letting

$$\mathbf{x} = (x_1, x_2), \quad \mathbf{p} = (r\cos(\theta), r\sin(\theta)),$$

the function u can be shown to satisfy the simplified equation

$$\mathcal{L}^2[u] \equiv u_t + c\cos(\theta)u_{x_1} + c\sin(\theta)u_{x_2} + (c_{x_1}\sin(\theta) - c_{x_2}\cos(\theta)) u_\theta = 0 \tag{4}$$

in "reduced phase-space" (x_1, x_2, θ). Similarly, in three dimensions we have

$$\begin{aligned}
\mathcal{L}^3[u] \equiv u_t &+ c\sin(\theta)\cos(\varphi)u_{x_1} + c\sin(\theta)\sin(\varphi)u_{x_2} + c\cos(\theta)u_{x_3} \\
&+ (c_{x_1}\cos(\theta)\cos(\varphi) + c_{x_2}\cos(\theta)\sin(\varphi) - c_{x_3}\sin(\theta)) u_\theta \\
&+ (c_{x_1}\sin(\varphi) - c_{x_2}\cos(\varphi)) \frac{u_\varphi}{\sin(\theta)} = 0 \quad (5)
\end{aligned}$$

where

$$\mathbf{x} = (x_1, x_2, x_3), \quad \mathbf{p} = (p_1, p_2, p_3) = (r\sin(\theta)\cos(\varphi), r\sin(\theta)\sin(\varphi), r\cos(\theta)). \tag{6}$$

As we anticipated, our use of the above phase-space formulation will follow the approach initiated in [23]. There it was recognized that the $d - 1$ dimensional wavefront in the $2d - 1$ dimensional reduced phase space $(d = 2, 3)$ can be simply identified through the intersection of level sets of d functions satisfying the corresponding reduced Liouville equation. Thus, within this context, the formulation of the geometrical optics evolution reduces to solving the (uncoupled) system of equations

$$\begin{cases} \mathcal{L}^2[u] = 0, \\ \mathcal{L}^2[v] = 0 \end{cases} \tag{7}$$

or

$$\begin{cases} \mathcal{L}^3[u] = 0, \\ \mathcal{L}^3[v] = 0, \\ \mathcal{L}^3[w] = 0 \end{cases} \tag{8}$$

in two and three dimensions respectively, where u, v, w are chosen to initially define the wavefront through the intersection of their zero level sets; the wavefront at later times is then recovered from analogous intersections [23]. Our scheme for the solution of (7), (8) is introduced in the next section.

3   A spectral/DGFEM formulation

The considerations in §2 reduce the problem of approximating the geometrical optics wavefront to that of approximating the (zero level set of the) solution of equations of the form (4) and (5). As we said, a main property of the Liouville formulation is that it unfolds the relevant multi-valued solutions which become *smooth* in phase space. In addition, for the problem at hand, the formulation entails a particularly simple dependence on the phase variables, which enter (4) and (5) in a straightforward multiplicative manner. To take advantage of these properties, we propose here a *spectral* method of solution. More precisely, in the two-dimensional case, we shall seek a solution $u = u(x_1, x_2, \theta, t)$ to (4) in the form of a (truncated) Fourier series

$$u(x_1, x_2, \theta, t) = \sum_{n=-N}^{N} U_n(x_1, x_2, t) \, e^{in\theta}. \tag{9}$$

Similarly, in three dimensions, we propose

$$u(x_1, x_2, x_3, \theta, \varphi, t) = \sum_{l=0}^{N} \sum_{m=-l}^{l} U_{l,m}(x_1, x_2, x_3, t) \, Y_l^m(\theta, \varphi) \tag{10}$$

where Y_l^m denotes the classical spherical harmonics. Our strategy entails the derivation of the system of equations satisfied *in physical space* by the coefficients in (9) and (10) and the design of a suitable high-order approximation scheme for the resulting problem. As we show next, the coefficients turn out to satisfy a rather simple (linear) hyperbolic system of equations. For such systems, in turn, high-order discontinuous Galerkin finite element methods [13,14] have been shown to be extremely effective, and a suitable DG approximation is presented in §3.2.

6

3.1 A hyperbolic system for the spectral coefficients

In this section we derive and analyze the system of equations satisfied by the coefficients in the spectral decomposition of the solution to the level set equation (4). For simplicity we shall present here the derivation and analysis for the two-dimensional case and the representation (9). Analogous, though somewhat more involved, calculations allow for the treatment of the corresponding system of equations in three dimensions for the coefficients in (10); see §6.

To derive the equations for U_n in (9) we begin by substituting the expansion into (4) to obtain

$$\sum_{n=-N}^{N} U_{n,t} \; e^{in\theta} + c \; \cos(\theta) \sum_{n=-N}^{N} U_{n,x_1} \; e^{in\theta} + c \; \sin(\theta) \sum_{n=-N}^{N} U_{n,x_2} \; e^{in\theta}$$

$$+ \left(c_{x_1} \; \sin(\theta) - c_{x_2} \; \cos(\theta) \right) \sum_{n=-N}^{N} in \; U_n e^{in\theta} = 0$$

or, equivalently,

$$\sum_{n=-N}^{N} U_{n,t} \; e^{in\theta} + \sum_{n=-N+1}^{N+1} \frac{c}{2} \; U_{n-1,x_1} \; e^{in\theta} + \sum_{n=-N-1}^{N-1} \frac{c}{2} \; U_{n+1,x_1} \; e^{in\theta}$$

$$+ \sum_{n=-N+1}^{N+1} \frac{(-ic)}{2} \; U_{n-1,x_2} \; e^{in\theta} + \sum_{n=-N-1}^{N-1} \frac{ic}{2} \; U_{n+1,x_2} \; e^{in\theta}$$

$$+ \sum_{n=-N+1}^{N+1} \frac{(-c_{x_2} - ic_{x_1})}{2} i(n-1) \; U_{n-1} \; e^{in\theta} + \sum_{n=-N-1}^{N-1} \frac{(-c_{x_2} + ic_{x_1})}{2} i(n+1) \; U_{n+1} \; e^{in\theta} = 0.$$

Setting

$$\mathbf{U} = \begin{bmatrix} U_{-N} \\ U_{-N+1} \\ \vdots \\ U_{N-1} \\ U_N \end{bmatrix} \in \mathbb{C}^{2N+1}$$

the last equation implies

$$\mathbf{U}_t + A_1 \mathbf{U}_{x_1} + A_2 \mathbf{U}_{x_2} + B\mathbf{U} = 0 \qquad (11)$$

7

where $A_1, A_2, B \in \mathbf{C}^{(2N+1)\times(2N+1)}$ are defined as

$$
A_1 = \begin{bmatrix}
0 & \frac{c}{2} & 0 & 0 & 0 & \cdots & 0 & 0 & 0 \\
\frac{c}{2} & 0 & \frac{c}{2} & 0 & 0 & \cdots & 0 & 0 & 0 \\
0 & \frac{c}{2} & 0 & \frac{c}{2} & 0 & \cdots & 0 & 0 & 0 \\
\vdots & \vdots & \vdots & \vdots & \vdots & \vdots & \vdots & \vdots & \vdots \\
0 & 0 & 0 & 0 & 0 & \cdots & \frac{c}{2} & 0 & \frac{c}{2} \\
0 & 0 & 0 & 0 & 0 & \cdots & 0 & \frac{c}{2} & 0
\end{bmatrix}, \tag{12}
$$

$$
A_2 = \begin{bmatrix}
0 & \frac{ic}{2} & 0 & 0 & 0 & \cdots & 0 & 0 & 0 \\
-\frac{ic}{2} & 0 & \frac{ic}{2} & 0 & 0 & \cdots & 0 & 0 & 0 \\
0 & -\frac{ic}{2} & 0 & \frac{ic}{2} & 0 & \cdots & 0 & 0 & 0 \\
\vdots & \vdots & \vdots & \vdots & \vdots & \vdots & \vdots & \vdots & \vdots \\
0 & 0 & 0 & 0 & 0 & \cdots & -\frac{ic}{2} & 0 & \frac{ic}{2} \\
0 & 0 & 0 & 0 & 0 & \cdots & 0 & -\frac{ic}{2} & 0
\end{bmatrix}, \tag{13}
$$

and

$$
B = \begin{bmatrix}
0 & (N-1)\frac{\gamma}{2} & 0 & 0 & 0 & \cdots & 0 & 0 & 0 \\
-N\frac{\overline{\gamma}}{2} & 0 & (N-2)\frac{\gamma}{2} & 0 & 0 & \cdots & 0 & 0 & 0 \\
0 & -(N-1)\frac{\overline{\gamma}}{2} & 0 & (N-3)\frac{\gamma}{2} & 0 & \cdots & 0 & 0 & 0 \\
\vdots & \vdots & \vdots & \vdots & \vdots & \vdots & \vdots & \vdots & \vdots \\
0 & 0 & 0 & 0 & 0 & \cdots & (N-2)\frac{\overline{\gamma}}{2} & 0 & -N\frac{\gamma}{2} \\
0 & 0 & 0 & 0 & 0 & \cdots & 0 & (N-1)\frac{\overline{\gamma}}{2} & 0
\end{bmatrix} \tag{14}
$$

and where we have set

$$
\gamma = \gamma(x_1, x_2) \equiv c_{x_1} + ic_{x_2}
$$

and have denoted its conjugate by $\overline{\gamma} \equiv c_{x_1} - ic_{x_2}$.

Clearly, from (12), (13), the equations (11) constitute a *symmetric hyperbolic system*. In fact, the system is strictly hyperbolic and explicitly diagonalizable. To see this, we begin by letting

$$
\boldsymbol{\nu} = (\nu_1, \nu_2) = \rho\left(\cos(\eta), \sin(\eta)\right)
$$

and we set

$$
A(\boldsymbol{\nu}) \equiv \nu_1 A_1 + \nu_2 A_2.
$$

8

Then, using (12), (13) we have

$$A(\boldsymbol{\nu}) = \rho A(\cos(\eta), \sin(\eta))$$

and we note that

$$P^{-1}A(\cos(\eta), \sin(\eta))P = A(1, 0) = A_1$$

where the $P = P(\eta)$ is a diagonal matrix with

$$P(\eta)_{jj} = e^{-ij\eta}. \tag{15}$$

Indeed, since

$$A(\cos(\eta), \sin(\eta))_{kl} = \frac{c}{2} \left[\delta_{k,l-1} e^{i\eta} + \delta_{k,l+1} e^{-i\eta} \right]$$

we have

$$\begin{aligned}
\left(P^{-1}A(\cos(\eta), \sin(\eta))P \right)_{pq} &= \frac{c}{2} \left[\delta_{p,q-1} e^{i\eta} + \delta_{p,q+1} e^{-i\eta} \right] e^{-i(q-p)\eta} \\
&= \frac{c}{2} \left[\delta_{p,q-1} + \delta_{p,q+1} \right] = (A_1)_{pq}.
\end{aligned}$$

Thus, we need only investigate the eigenvalues and eigenvectors of the matrix A_1. As can be easily checked, however, the eigenvalues λ_j are simply given by

$$\lambda_j = \lambda_j(x_1, x_2) = c(x_1, x_2) \cos\left(\frac{j\pi}{2(N+1)} \right), \quad j = 1, \cdots, 2N+1, \tag{16}$$

with a corresponding normalized eigenvector

$$\mathbf{v}_j = \frac{1}{\sqrt{N+1}} \begin{bmatrix} \sin(\frac{j\pi}{2(N+1)}) \\ \sin(\frac{2j\pi}{2(N+1)}) \\ \vdots \\ \sin(\frac{2Nj\pi}{2(N+1)}) \\ \sin(\frac{(2N+1)j\pi}{2(N+1)}) \end{bmatrix}. \tag{17}$$

As a result, letting

$$V = \left[\mathbf{v}_1 \mathbf{v}_2 \cdots \mathbf{v}_{2N+1} \right] \in \mathbb{C}^{(2N+1) \times (2N+1)}$$

and

$$\Lambda = \mathrm{diag}(\lambda_1, \lambda_2, \cdots, \lambda_{2N+1})$$

we have

$$A(\cos(\eta), \sin(\eta)) = S(\eta)\Lambda S(\eta)^{-1} \tag{18}$$

9

where
$$S(\eta) = P(\eta)V \quad \text{and} \quad S(\eta)^{-1} = V^T \, \overline{P(\eta)}. \tag{19}$$
Finally, we note that, from (16), there are exactly N positive and N negative eigenvalues,

$$\lambda_1 > \lambda_2 > \cdots > \lambda_N > \lambda_{N+1} = 0 > \lambda_{N+2} > \lambda_{N+3} > \cdots > \lambda_{2N+1}$$

so that the matrix A can be decomposed as

$$A(\cos(\eta), \sin(\eta)) = A^+(\cos(\eta), \sin(\eta)) + A^-(\cos(\eta), \sin(\eta)) \tag{20}$$

where
$$A^{\pm}(\cos(\eta), \sin(\eta)) = S(\eta)\Lambda^{\pm}S(\eta)^{-1}$$
and

$$\Lambda^+ = \text{diag}(\lambda_1, \lambda_2, \cdots, \lambda_N, 0, \cdots, 0), \quad \Lambda^- = \text{diag}(0, \cdots, 0, \lambda_{N+2}, \lambda_{N+3}, \cdots, \lambda_{2N+1}).$$

3.2 Discontinuous Galerkin approximation

As we said, the hyperbolic nature of the system (11) makes it amenable to a high-order treatment via discontinuous Galerkin finite element methods [13,14]. In order to specify the details of the DG scheme we propose to approximate the system, we begin by re-writing it in "conservation form", that is
$$\mathbf{U}_t + \text{div}\,(\mathbf{F}(\mathbf{U})) + C\mathbf{U} = 0 \tag{21}$$
where
$$\mathbf{F}(\mathbf{U}) = \left[A_1\mathbf{U}, A_2\mathbf{U} \right]$$
and
$$C = B - \partial_{x_1}A_1 - \partial_{x_2}A_2$$
or, explicitly,

$$C = \begin{bmatrix} 0 & (N-2)\frac{\gamma}{2} & 0 & 0 & 0 \cdots & 0 & 0 & 0 \\ -(N+1)\frac{\overline{\gamma}}{2} & 0 & (N-3)\frac{\gamma}{2} & 0 & 0 \cdots & 0 & 0 & 0 \\ 0 & -N\frac{\overline{\gamma}}{2} & 0 & (N-4)\frac{\gamma}{2} & 0 \cdots & 0 & 0 & 0 \\ \vdots & \vdots & \vdots & \vdots & \vdots \; \vdots & \vdots & \vdots & \vdots \\ 0 & 0 & 0 & 0 & 0 \cdots & (N-3)\frac{\overline{\gamma}}{2} & 0 & -(N+1)\frac{\gamma}{2} \\ 0 & 0 & 0 & 0 & 0 \cdots & 0 & (N-2)\frac{\overline{\gamma}}{2} & 0 \end{bmatrix} \tag{22}$$

Next, to approximate the system (21) we consider a partition $T_h = \{K_n\}$ of a computational domain Ω and local spaces $P^k(K_n)$ on each element K_n consisting of polynomials of degree smaller than or equal to k. Then, expanding

$$\mathbf{U}_h\Big|_{K_n} = \sum_{j=1}^{N_k} \psi_j(\mathbf{x})\mathbf{c}_j^{K_n}(t), \tag{23}$$

in terms of basis functions $\psi_j \in P^k(K)$, a DG formulation takes on the form

$$\int_{K_n} \frac{\partial \mathbf{U}_h}{\partial t}\psi\, dx - \int_{K_n} \mathbf{F}(\mathbf{U}_h)\cdot\nabla\psi\, dx + \int_{K_n} C\mathbf{U}_h\psi\, dx + \int_{\partial K_n} \widehat{\mathbf{F}_h}\cdot\boldsymbol{\nu}\psi\, ds = 0, \tag{24}$$

for all $\psi \in P^k(K_n)$, where $\boldsymbol{\nu}$ is the outward unit normal vector to ∂K_n and $\widehat{\mathbf{F}_h} \cdot \boldsymbol{\nu}$ is the *numerical flux* on ∂K_n [14]. As is well known the appropriate choice of these numerical fluxes constitutes a central component within these schemes. For linear hyperbolic problems a natural choice is that corresponding to "upwinding", wherein information travels along local wave directions. For the present case, and on account of (20), the upwind flux can be written as

$$\widehat{\mathbf{F}_h}\cdot\boldsymbol{\nu} = A^+(\cos(\eta),\sin(\eta))\mathbf{U}_h^+ + A^-(\cos(\eta),\sin(\eta))\mathbf{U}_h^- \tag{25}$$

where $\mathbf{U}_h^\pm$ denote the inner and outer values of $\mathbf{U}_h$ on ∂K_n respectively, and

$$\boldsymbol{\nu} = (\cos(\eta),\sin(\eta)). \tag{26}$$

Clearly, the outer values $\mathbf{U}_h^-$ must be properly defined for elements K_n whose boundary intersects that of the computational domain Ω. The precise definition of these values will, of course, depend on the boundary conditions whose treatment we defer to the next section. In any case, substituting the expansion (23) into the formulation (24) leads to a linear system of ordinary differential equations for the coefficients $\mathbf{c}_j^{K_n}(t)$ which must be integrated in time. For this we resort to the mth-order, m-stage strong stability preserving Runge-Kutta (SSP-RK) scheme with low storage introduced in [19]. This addition completes our overall strategy in a manner that, as we said, enables calculations of arbitrarily high order while, at the same time, allowing for general geometrical arrangements.

4   Boundary conditions: reflecting and absorbing boundaries

As we said, the definition of the exterior values $\mathbf{U}_h^-$ to be used in the numerical flux (25) must be properly defined for elements intersecting the boundary of Ω. In the case of absorbing boundaries (as necessary, for instance, in scattering simulations) this definition is rather straightforward: in this case, we may simply define

$$\mathbf{U}_h^- = \mathbf{U}_h^+ \tag{27}$$

to approximate an outflow boundary.

The incorporation of reflecting boundaries, on the other hand, requires further developments based, of course, on the geometrical optics "law of reflection". We recall [7] that this principle asserts that at a reflecting interface Γ we must have

$$\text{incident angle} = \text{reflected angle} \tag{28}$$

where the incident and reflected angles are defined as the angles between the incident and reflected rays and the outward normal vector to Γ respectively. More precisely, if θ_{inc} and θ_{refl} denote the polar angles of the incident and reflected rays, and if η denotes that of the normal vector, equation (28) can be written as

$$\theta_{\text{inc}} + \pi - \eta = \eta - \theta_{\text{refl}}$$

that is

$$\theta_{\text{refl}} = 2\eta - \pi - \theta_{\text{inc}}. \tag{29}$$

This last equation can be used to impose a boundary condition on the level set function u in (9) in the form

$$u(x_1, x_2, \theta, t) = u(x_1, x_2, 2\eta - \pi - \theta, t) \quad \text{for } \mathbf{x} \in \Gamma, \ \theta \in [0, 2\pi]. \tag{30}$$

To incorporate this condition into our scheme, however, we must derive from it a relation on the Fourier coefficients U_n which should, in turn, lead to a suitable definition of $\mathbf{U}_h^-$ in (25).

To derive this definition we begin by noting that, in terms of Fourier coefficients, the boundary condition (30) translates to

$$U_{-n}(\mathbf{x}, t) = e^{in(2\eta - \pi)} U_n(x_1, x_2, t) \ \text{for } \mathbf{x} \in \Gamma, \quad n = 1, \cdots, N,$$

This last relation, in turn, can be written as

$$\mathcal{B}\mathbf{U}(\mathbf{x}, t) = 0, \quad \mathbf{x} \in \Gamma, \tag{31}$$

where

$$\mathcal{B} = \mathcal{B}(\eta) = \begin{bmatrix} 1 & 0 & 0 & \cdots & 0 & 0 & 0 & 0 & 0 & 0 & \cdots & 0 & 0 & -\alpha^N \\ 0 & 1 & 0 & \cdots & 0 & 0 & 0 & 0 & 0 & 0 & \cdots & 0 & -\alpha^{N-1} & 0 \\ \vdots & \vdots & \vdots & \vdots & \vdots & \vdots & \vdots & \vdots & \vdots & \vdots & \vdots & \vdots & \vdots & \vdots \\ 0 & 0 & 0 & \cdots & 1 & 0 & 0 & 0 & -\alpha^2 & 0 & \cdots & 0 & 0 & 0 \\ 0 & 0 & 0 & \cdots & 0 & 1 & 0 & -\alpha & 0 & 0 & \cdots & 0 & 0 & 0 \end{bmatrix} \in \mathbb{C}^{N \times (2N+1)} \tag{32}$$

and

$$\alpha = e^{in(2\eta - \pi)}.$$

12

At this point, we note that the conditions in (31) are correct in number, as the system possesses precisely N incoming characteristic directions (corresponding to the N negative eigenvalues in (16)). To justify the well-posedness of the problem (11) subject to (32), however, we must further verify that (31) leads to an equation that allows for the determination of the incoming part of the solution in terms of the outgoing portion. More precisely, at any point $\mathbf{x} \in \Gamma$ with normal $\boldsymbol{\nu} = (\cos(\eta), \sin(\eta))$, we consider the normalized eigenvectors $\mathbf{s}_j$ of $A(\cos(\eta), \sin(\eta))$ (cf. (18)) corresponding to the eigenvalues λ_j in (16), $j = 1, \cdots, 2N+1$. Then, the projection onto the space of outgoing directions is given by

$$\Pi^+ = S^+ (S^+)^T$$

where

$$S^+ = S^+(\eta) = [\mathbf{s}_1 \cdots \mathbf{s}_N],$$

while that onto the incoming directions is

$$\Pi^- = S^- (S^-)^T$$

with

$$S^- = S^-(\eta) = [\mathbf{s}_{N+2} \cdots \mathbf{s}_{2N+1}]$$

and the condition (31) can be interpreted as providing values for $\Pi^- \mathbf{U}$ from knowledge of $\Pi^+ \mathbf{U}$. Indeed, from (31) we have

$$0 = \mathcal{B}\mathbf{U} = \mathcal{B}\Pi^- \mathbf{U} + \mathcal{B}(I - \Pi^-)\mathbf{U}$$

or, equivalently,

$$\mathcal{B}S^- \left[(S^-)^T \mathbf{U} \right] = -\mathcal{B}(I - \Pi^-)\mathbf{U}. \tag{33}$$

As we show in Appendix A, the matrix $\mathcal{B}S^- \in \mathbb{C}^{N \times N}$ is (explicitly) invertible. Thus, from (33)

$$(S^-)^T \mathbf{U} = - \left(\mathcal{B}S^- \right)^{-1} \mathcal{B}(I - \Pi^-)\mathbf{U}.$$

and therefore

$$\Pi^- \mathbf{U} = -S^- \left(\mathcal{B}S^- \right)^{-1} \mathcal{B}(I - \Pi^-)\mathbf{U} \tag{34}$$

which provides incoming values for $\mathbf{U}$ in terms of its outgoing (and stationary) projection. Finally, and on account of (34), at a reflecting boundary Γ we define the numerical flux as in (25) where

$$\mathbf{U}_h^- = -S^- \left(\mathcal{B}S^- \right)^{-1} \mathcal{B}(I - \Pi^-)\mathbf{U}_h^+. \tag{35}$$

5   Numerical examples

In this section we present a few numerical results from an implementation of the two-dimensional scheme (in three-dimensional reduced phase space)

described above in the case $c \equiv \text{const.} \equiv 1$. In this connection, our first set of experiments are designed to confirm the accuracy of the implementation of both the interior scheme as well as that of the boundary conditions. While simple exact solutions to (4) can be easily derived (e.g. $u(\mathbf{x}, \mathbf{p}, t) = x_1 - c\cos(\theta)t$), the derivation of explicit solutions satisfying reflecting or absorbing boundary conditions is not straightforward. To bypass this problem while providing a full assessment of the quality of the approximations generated by our proposed procedure, we have tested the method on the function

$$u(\mathbf{x}, \theta, t) = \sin(3\pi x_1)\sin(4\pi x_2)\sin(\frac{\pi}{2}t)\frac{1}{(1 + \cos(2\theta)^2)}. \tag{36}$$

defined in the computational domain $\Omega = [-1, 1] \times [-1, 1]$. This function presents several desirable attributes for the testing of our algorithms: it is oscillatory, not exactly representable by a finite polynomial expansion and its spectral representation in phase space also leads to an infinite series. In addition, the specific form of the dependence in θ guarantees that it also satifies the reflecting boundary condition (30) over all of $\partial\Omega$.

The function in (36), however, *does not* solve the homogeneous equation (4). Still, it can be viewed as solving its (slightly more complex) inhomogeneous version

$$\mathcal{L}^2[u] \equiv u_t + c\cos(\theta)u_{x_1} + c\sin(\theta)u_{x_2} + (c_{x_1}\sin(\theta) - c_{x_2}\cos(\theta))\,u_\theta = G(\mathbf{x}, \theta, t) \tag{37}$$

for an appropriately defined function G. Clearly, the numerical procedure outlined in §3 extends rather straightforwardly, for the most part, to the solution of (37). An exception, however, is the time integration strategy which, as described, applies only to homogeneous systems of ordinary differential equations. As follows from (37) though, in this case the coefficients $\mathbf{c}_j^{K_n}(t)$ in (23) satisfy an inhomogeneous system, whose solution demands a suitable extension of the SSP-RK integrator in [19] alluded to in §3.2. One such extension was recently introduced in [10] where its high-order convergence characteristics were demonstrated. More precisely, if a version of order $k + 1$ of this extended SSP-RK method is used to integrate the equations that result from a DG formulation with polynomials of degree k, the overall scheme will converge with order $k + 1$ provided that the CFL condition

$$\Delta t \leq \frac{h}{2\,k + 1} \tag{38}$$

is satisfied. With this time integrator (which, as we said, reduces to that of [19] in the absence of source terms) the results of our overall approximation procedure to the solution (36) of (37) are presented in Table 1 and Figure 1. More precisely, in Table 1 we show that, indeed, our implementation converges with the correct orders in space and time. Figure 1, on the other hand, shows

14

that spectral convergence is attained in both the p-version of the finite element method, as well as in the phase variable.

Table 1
Convergence results for different space-time approximation orders for the solution (36) at $t = 1$. The spatial meshes are successively refined by a factor of two and they contain 2, 8, 32, 128, 512, 2048 and 8192 elements, respectively; in every case, the time-step is taken to be proportional to the size of the spatial discretization, and to satisy the CFL condition (38).

$N = 40$; P^1; SSP-RK2				$N = 40$; P^2; SSP-RK3		
h	L^2-error	Order		h	L^2-error	Order
2.83E+00	3.02E+00	–		2.83E+00	4.93E+00	–
1.41E+00	3.72E+00	-0.30		1.41E+00	5.40E+00	-0.13
7.07E-01	1.64E+00	1.18		7.07E-01	1.48E+00	1.87
3.54E-01	1.18E+00	0.48		3.54E-01	4.77E-01	1.63
1.77E-01	4.12E-01	1.52		1.77E-01	6.69E-02	2.83
8.84E-02	1.04E-01	1.99		8.84E-02	8.34E-03	3.00
4.42E-02	2.38E-02	2.12		4.42E-02	1.03E-03	3.02

$N = 40$; P^3; SSP-RK4				$N = 40$; P^4; SSP-RK5		
h	L^2-error	Order		h	L^2-error	Order
2.83E+00	6.84E+00	–		2.83E+00	7.36E+00	–
1.41E+00	5.74E+00	0.25		1.41E+00	5.99E+00	0.30
7.07E-01	9.93E-01	2.53		7.07E-01	6.84E-01	3.13
3.54E-01	1.57E-01	2.66		3.54E-01	3.57E-02	4.26
1.77E-01	1.15E-02	3.77		1.77E-01	1.43E-03	4.64
8.84E-02	7.07E-04	4.02		8.84E-02	4.53E-05	4.98

The final examples are concerned with true solutions to (7) in $\Omega = [-1, 1] \times [-1, 1]$ generated by a point source located at the origin, and subject to reflecting and absorbing boundary conditions. In Figure 2 we display the actual physical wavefront in Ω at different times for a case where all boundaries are perfect reflectors; the results correspond to a truncation parameter $N = 40$, an approximation with polynomials of degree four (P^4) and a time-integration of order five (SSP-RK5) on a coarse grid with 8 elements ($h = 1.41$). The fronts in Figure 2 are, of course, the projection of the phase-space wavefronts which are, in turn, defined as the intersection of the zero level sets of u and v in (7). Clearly, a number of alternative strategies are possible to determine these

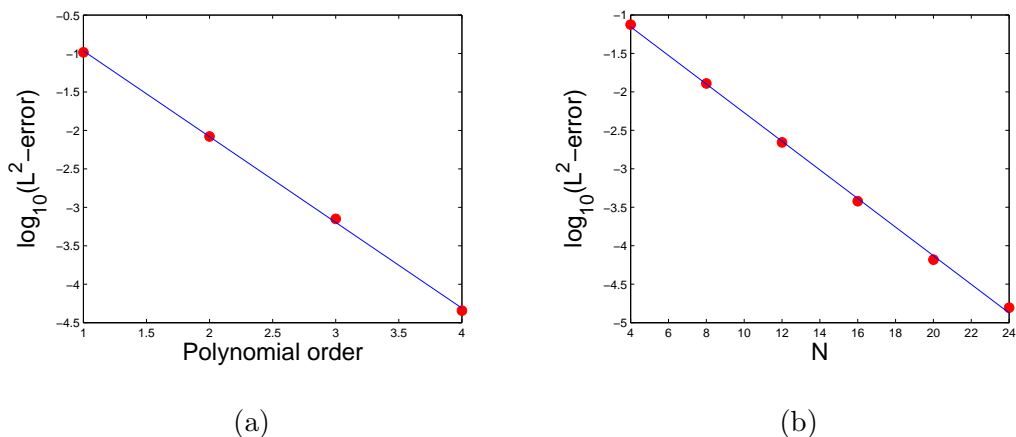(a)   (b)

Fig. 1. Spectral convergence of the scheme to the solution (36) at $t = 1$: (a) convergence in polynomial order k in the spatial representation –disks– and best linear fit –line– (h=8.84E-02, $N = 40$); (b) convergence in truncation parameter N in the spectral representation of the phase variables –disks– and best linear fit –line– (h=4.42E-02, $k = 4$).

level sets and their intersections; for simplicity, for this and the examples that follow, these calculations were performed, in a post-processing stage, via linear approximations on a much refined grid in phase space. The level sets and their intersection at the time corresponding to the most advanced front in Figure 2 ($t = 1.3$) are shown in Figure 3(a) and Figure 3(b) respectively.
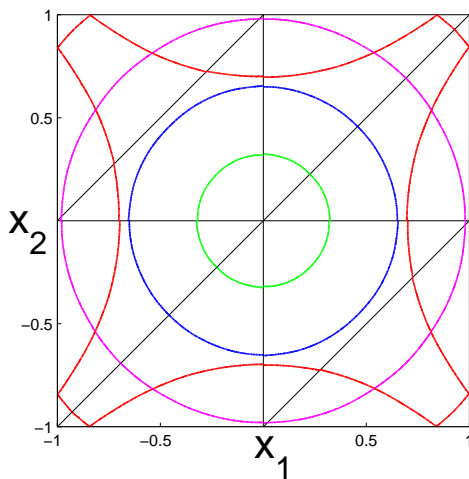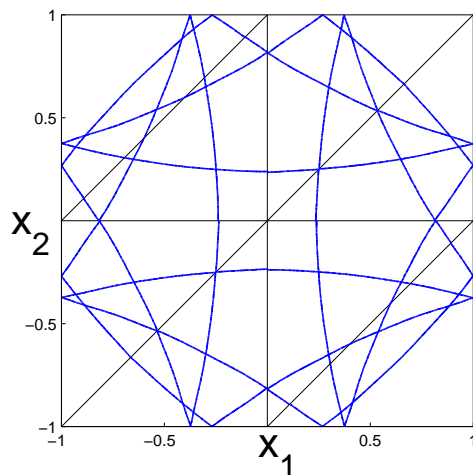

Fig. 2. Reflecting boundaries: projection onto physical space of the wavefront generated by a point source at $(0,0)$ at $t = 0.325, 0.65, 0.975$ and 1.3 (note the 8-element spatial mesh in the background).

As we have said, a central characteristic of phase-space methodologies is their ability to capture multi-valued solutions of the eikonal equation. An example of this situation is presented in Figure 4 which again corresponds to a domain with perfectly reflecting boundaries ($N = 40$, h=1.41, $k = 4$ and SSP-RK5);

16

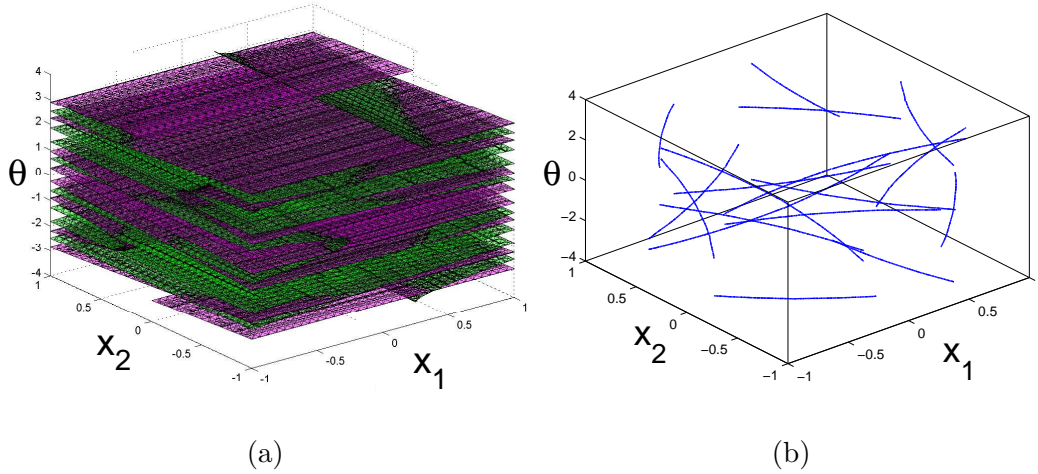(a)   (b)
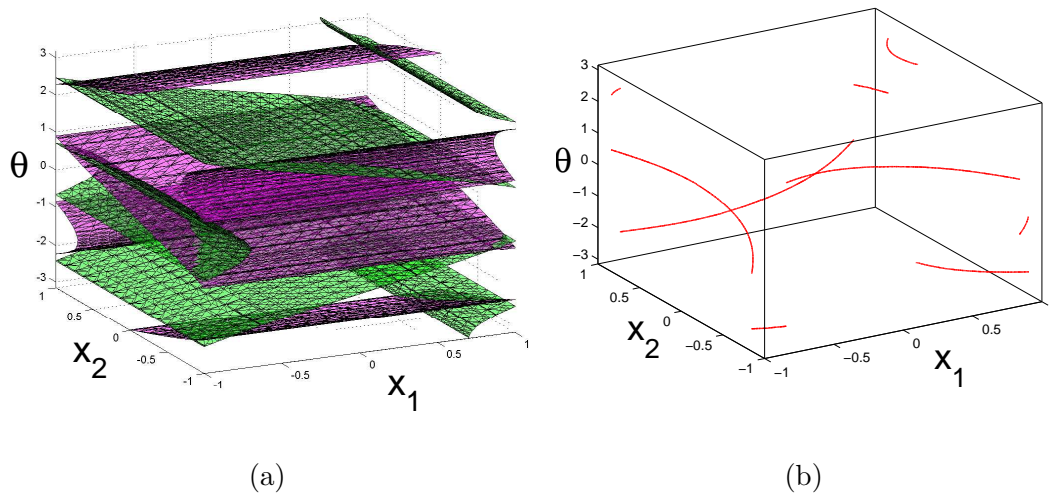
Fig. 3. Zero level sets in reduced phase space for the example in Fig. 2: (a) zero level sets of u and v at $t = 1.3$; (b) intersection of level sets in (a) defining the wavefront in phase space (note that the corresponding curve in Fig. 2 —$t = 1.3$— coincides precisely with the projection of this wavefront).

the corresponding zero level sets of u and v and their intersection are depicted in Figure 5. Finally, Figure 6 shows an instance of a domain with absorbing boundaries. Indeed, to exemplify the versatility afforded by the nature of our boundary treatment (based simply on the choice of numerical fluxes), we display the results on a domain that combines absorbing boundaries at $x_1 = -1$, $x_2 = \pm 1$ with a reflecting boundary at $x_1 = 1$.

Fig. 4. Reflecting boundaries: projection onto physical space of the wavefront generated by a point source at $(0, 0)$ at $t = 3.75$ corresponding to a multi-valued solution of the eikonal equation (note the 8-element spatial mesh in the background).

17

(a)   (b)

Fig. 5. Zero level sets in reduced phase space for the example in Fig. 4: (a) zero level sets of u and v at $t = 3.75$; (b) intersection of level sets in (a) defining the wavefront in phase space (again here, the curve in Fig. 4 corresponds precisely to the projection of this wavefront onto physical space).
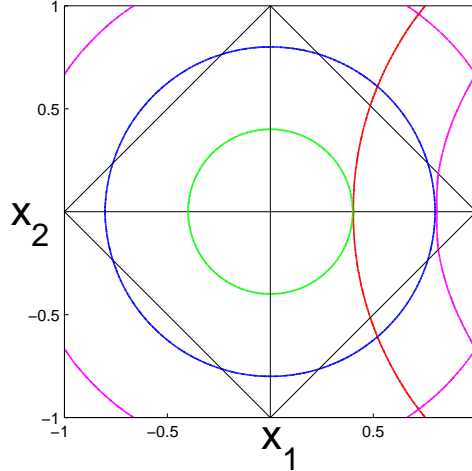

Fig. 6. Reflecting/Absorbing boundaries: projection onto physical space of the wavefront generated by a point source at $(0,0)$ at $t = 0.4, 0.8, 1.2$ and 1.6 (note the 8-element spatial mesh in the background).

6   Extensions and improvements

As we argued in §3, the spectral/DG formulation readily extends to configurations in three space dimensions. In this case, as we mentioned, we seek a solution in the form (10) where the spherical harmonics Y_l^m are defined as

$$Y_l^m(\theta, \varphi) = (-1)^m \sqrt{\frac{(2l+1)}{4\pi} \frac{(l-m)!}{(l+m)!}} P_l^m(\cos(\theta)) e^{im\varphi}$$

18

and P_l^m are the associated Legendre functions. To derive the analogue of (11) in this case, we shall need the classical formulas for the gradient of the spherical harmonics: letting $\mathbf{p}$ be as in (6) we have

$$r\left(\frac{\partial}{\partial p_1} + i\frac{\partial}{\partial p_2}\right)Y_l^m = l\sqrt{\frac{(l+m+2)(l+m+1)}{(2l+3)(2l+1)}}Y_{l+1}^{m+1} + (l+1)\sqrt{\frac{(l-m)(l-m-1)}{(2l+1)(2l-1)}}Y_{l-1}^{m+1}$$

$$r\left(-\frac{\partial}{\partial p_1} + i\frac{\partial}{\partial p_2}\right)Y_l^m = l\sqrt{\frac{(l-m+2)(l-m+1)}{(2l+3)(2l+1)}}Y_{l+1}^{m-1} + (l+1)\sqrt{\frac{(l+m)(l+m-1)}{(2l+1)(2l-1)}}Y_{l-1}^{m-1}$$

$$r\frac{\partial}{\partial p_3}Y_l^m = -l\sqrt{\frac{(l+m+1)(l-m+1)}{(2l+3)(2l+1)}}Y_{l+1}^m + (l+1)\sqrt{\frac{(l+m)(l-m)}{(2l+1)(2l-1)}}Y_{l-1}^m.$$

From these, it follows that

$$r\frac{\partial}{\partial p_j}Y_l^m = \sum_{\substack{l-1\leq l'\leq l+1 \\ m-1\leq m'\leq m+1}} b_{lm,l'm'}^j Y_{l'}^{m'} \tag{39}$$

for suitably defined constants $b_{lm,l'm'}^j$. In addition, we shall need the expressions for the basic local multiplicative operators:

$$\cos(\theta)Y_l^m = \sqrt{\frac{(l+m+1)(l-m+1)}{(2l+3)(2l+1)}}Y_{l+1}^m + \sqrt{\frac{(l+m)(l-m)}{(2l+1)(2l-1)}}Y_{l-1}^m$$

$$\sin(\theta)e^{i\varphi}Y_l^m = -\sqrt{\frac{(l+m+2)(l+m+1)}{(2l+3)(2l+1)}}Y_{l+1}^{m+1} + \sqrt{\frac{(l-m)(l-m-1)}{(2l+1)(2l-1)}}Y_{l-1}^{m+1}$$

$$\sin(\theta)e^{-i\varphi}Y_l^m = \sqrt{\frac{(l-m+2)(l-m+1)}{(2l+3)(2l+1)}}Y_{l+1}^{m-1} - \sqrt{\frac{(l+m)(l+m-1)}{(2l+1)(2l-1)}}Y_{l-1}^{m-1}$$

from which we deduce

$$\sin(\theta)\cos(\varphi)Y_l^m = \sum_{\substack{l-1\leq l'\leq l+1 \\ m-1\leq m'\leq m+1}} a_{lm,l'm'}^1 Y_{l'}^{m'}$$

$$\sin(\theta)\sin(\varphi)Y_l^m = \sum_{\substack{l-1\leq l'\leq l+1 \\ m-1\leq m'\leq m+1}} a_{lm,l'm'}^2 Y_{l'}^{m'} \tag{40}$$

$$\cos(\theta)Y_l^m = \sum_{\substack{l-1\leq l'\leq l+1 \\ m-1\leq m'\leq m+1}} a_{lm,l'm'}^3 Y_{l'}^{m'}$$

for some constants $a_{lm,l'm'}^j$. Then, substituting the expression (10) into (5) we obtain

$$
\sum_{l,m} U_{lm,t} Y_l^m - \sum_{l,m} U_{lm} \left[c_{x_1} r \frac{\partial Y_l^m}{\partial p_1} + c_{x_2} r \frac{\partial Y_l^m}{\partial p_2} + c_{x_3} r \frac{\partial Y_l^m}{\partial p_3} \right]
$$
$$
+ \sum_{l,m} c \left[U_{lm,x_1} \sin(\theta) \cos(\varphi) Y_l^m + U_{lm,x_2} \sin(\theta) \sin(\varphi) Y_l^m + U_{lm,x_3} \cos(\theta) Y_l^m \right] = 0
$$

which, using (39) and (40), implies

$$
U_{lm,t} + \sum_{\substack{l-1 \le l' \le l+1 \\ m-1 \le m' \le m+1}} c \left[a_{l'm',lm}^1 U_{l'm',x1} + a_{l'm',lm}^2 U_{l'm',x2} + a_{l'm',lm}^3 U_{l'm',x3} \right]
$$
$$
\sum_{\substack{l-1 \le l' \le l+1 \\ m-1 \le m' \le m+1}} U_{l'm'} \left[c_{x_1} b_{l'm',lm}^1 + c_{x_2} b_{l'm',lm}^2 + c_{x_3} b_{l'm',lm}^3 \right] = 0 \quad (41)
$$

for (l,m) such that $|m| \le l$ and $0 \le l \le N$. Clearly, in matrix form, the equations (41) can be written as

$$
\mathbf{U}_t + A_1 \mathbf{U}_{x_1} + A_2 \mathbf{U}_{x_2} + A_3 \mathbf{U}_{x_3} + B\mathbf{U} = 0 \quad (42)
$$

where A_j, B are sparse matrices with nonzero entries defined as

$$
(A_j)_{lm,l'm'} = c\, a_{l'm',lm}^j
$$
$$
B_{lm,l'm'} = \sum_{j=1}^3 c_{x_j}\, b_{l'm',lm}^j.
$$

Note that the formulation (42) possesses an additional advantage over that in (5) as it naturally resolves the –artificial– singularities at the poles that are introduced when using spherical coordinates to resolve phase variables; compare [23, Sec. 7].

Finally, a number of improvements in the numerical implementation are also possible. For instance, *high-order* localization and reinitialization could be included, e.g. along the lines of those proposed in [30]; see also [24]. Also, higher-order schemes for the intersection of multi-dimensional level sets can be devised to take full advantage of the accuracy of the spectral-DG solutions. The numerical implementation of these, as that of the three-dimensional system (42), will, however, be left for future work.

A An expression for the outer flux on reflection

In this Appendix we show that the matrix $(\mathcal{B}S^-)^{-1}$ appearing in (34) and (35) can be computed explicitly. To this end, we begin by showing that the dependence of $\mathcal{B}S^-$ on the polar angle η can be reduced to multiplication by a diagonal matrix. Indeed, from (32), we have

$$\mathcal{B}_{kj} = \mathcal{B}(\eta)_{kj} = \delta_{k,j} - \delta_{k,2(N+1)-j}(-1)^{N+1-k}e^{i2\eta(N+1-k)} \qquad (A.1)$$

so that, using (15),

$$
\begin{aligned}
(\mathcal{B}(\eta)P(\eta))_{kj} &= \sum_{l=1}^{2N+1} \mathcal{B}_{kl}\delta_{l,j}e^{-ij\eta} \\
&= \sum_{l=1}^{2N+1} \left[\delta_{k,l}\delta_{l,j}e^{-ij\eta} - \delta_{k,2(N+1)-l}(-1)^{N+1-k}e^{i2\eta(N+1-k)}\delta_{l,j}e^{-ij\eta} \right] \\
&= \delta_{k,j}e^{-ij\eta} - \delta_{k,2(N+1)-j}(-1)^{N+1-k}e^{i2\eta(N+1-k)}e^{-ij\eta} \\
&= \delta_{k,j}e^{-ij\eta} - \delta_{k,2(N+1)-j}(-1)^{N+1-k}e^{i2\eta(N+1-k)}e^{-i(2(N+1)-k))\eta} \\
&= \delta_{k,j}e^{-ik\eta} - \delta_{k,2(N+1)-j}(-1)^{N+1-k}e^{-ik\eta} = e^{-ik\eta}\mathcal{B}(0)_{kj}
\end{aligned}
$$

that is,

$$\mathcal{B}(\eta)P(\eta) = \mathrm{diag}(e^{-i\eta}, e^{-i2\eta}, \cdots, e^{-iN\eta})\mathcal{B}(0). \qquad (A.2)$$

On the other hand, using (15), (19), we have

$$S^-(\eta) = P(\eta)S^-(0)$$

and therefore, from (A.2),

$$\mathcal{B}(\eta)S^-(\eta) = \mathcal{B}(\eta)P(\eta)S^-(0) = \mathrm{diag}(e^{-i\eta}, e^{-i2\eta}, \cdots, e^{-iN\eta})\mathcal{B}(0)S^-(0) \quad (A.3)$$

where

$$S^-(0) = [\mathbf{v}_{N+2} \cdots \mathbf{v}_{2N+1}]$$

with $\mathbf{v}_j$ as in (17). Equation (A.3) then reduces the problem of inverting $\mathcal{B}(\eta)S^-(\eta)$ to that of inverting the matrix $M \in \mathbb{C}^{N \times N}$ defined as

$$M = \mathcal{B}(0)S^-(0).$$

To invert this matrix, in turn, we first note that from (A.1) and (17)

$$
\begin{aligned}
M_{kj} &= \frac{1}{\sqrt{N+1}} \sum_{l=1}^{N} \left(\delta_{k,l} - \delta_{k,2(N+1)-l}(-1)^{N+1-k}\right) \sin(\frac{l(j+N+1)\pi}{2(N+1)}) \\
&= \frac{1}{\sqrt{N+1}} \left(\sin(\frac{k(j+N+1)\pi}{2(N+1)}) - (-1)^{N+1-k} \sin(\frac{(2(N+1)-k)(j+N+1)\pi}{2(N+1)})\right) \\
&= \frac{1}{\sqrt{N+1}} \left(\sin(\frac{k(j+N+1)\pi}{2(N+1)}) + (-1)^{N+1-k}(-1)^{j+N+1} \sin(\frac{k(j+N+1)\pi}{2(N+1)})\right) \\
&= \frac{1}{\sqrt{N+1}} \left(1 + (-1)^{j+k}\right) \sin(\frac{k(j+N+1)\pi}{2(N+1)}).
\end{aligned}
$$

In particular, we have that $M_{kj} \neq 0$ only if $k+j$ is even. Thus, letting

$$L = \left[\frac{N}{2}\right], \quad K = N - L,$$

we define new matrices $M_1 \in \mathbb{C}^{L \times L}$ and $M_2 \in \mathbb{C}^{K \times K}$ by

$$(M_1)_{kj} = M_{2k,2j} \quad \text{and} \quad (M_2)_{kj} = M_{2k-1,2j-1}.$$

As it turns out, the inverse matrix M^{-1} can be easily computed from knowledge of the inverses of M_1 and M_2; and, moreover, these latter matrices are *orthogonal*, $M_j^{-1} = M_j^T$. Indeed, letting

$$
R_{kj} = \begin{cases}
0 & \text{if } k+j \text{ is odd,} \\
(M_1^{-1})_{\frac{k}{2},\frac{j}{2}} & \text{if } k \text{ and } j \text{ are even,} \\
(M_2^{-1})_{\frac{k+1}{2},\frac{j+1}{2}} & \text{if } k \text{ and } j \text{ are odd,}
\end{cases} \quad (A.4)
$$

we have

$$(MR)_{kj} = \sum_{l=1}^{N} M_{kl} R_{lj} = \sum_{l=1}^{L} M_{k,2l} R_{2l,j} + \sum_{l=1}^{K} M_{k,2l-1} R_{2l-1,j}$$

$$= \begin{cases} 0 & \text{if } k+j \text{ is odd,} \\ \sum_{l=1}^{L} (M_1)_{\frac{k}{2},l}(M_1^{-1})_{l,\frac{j}{2}} & \text{if } k \text{ and } j \text{ are even,} \\ \sum_{l=1}^{K} (M_2)_{\frac{k+1}{2},l}(M_2^{-1})_{l,\frac{j+1}{2}} & \text{if } k \text{ and } j \text{ are odd,} \end{cases}$$

$$= \delta_{k,j}$$

that is

$$R = M^{-1}.$$

Finally, we show that the matrix M_1 is orthogonal; the orthogonality of M_2 can be similarly establish. For the sake of definiteness, we shall assume that N is even so that

$$L = \frac{N}{2};$$

the case $L = (N-1)/2$ (N odd) can be treated in an entirely analogous way. Under this assumption then we have

$$\sum_{l=1}^{L} (M_1)_{lk}(M_1)_{lj} = \sum_{l=1}^{L} M_{2l,2k} M_{2l,2j}$$

$$= \frac{4}{N+1} \sum_{l=1}^{L} \sin\left(\frac{2l(2k+N+1)\pi}{2(N+1)}\right) \sin\left(\frac{2l(2j+N+1)\pi}{2(N+1)}\right)$$

$$= \frac{4}{N+1} \sum_{l=1}^{L} \sin\left(\frac{2lk\pi}{N+1}\right) \sin\left(\frac{2lj\pi}{N+1}\right)$$

$$= \frac{2}{N+1} \sum_{l=1}^{L} \left[\cos\left(\frac{2l(k-j)\pi}{N+1}\right) - \cos\left(\frac{2l(k+j)\pi}{N+1}\right)\right]$$

and using

$$\sum_{l=1}^{L} \cos(2lx) = \frac{1}{2}\left[\cos(Nx) - 1 + \sin(Nx)\,\text{cotg}(x)\right] \qquad (A.5)$$

we obtain

$$\sum_{l=1}^{L} (M_1)_{lk}(M_1)_{lj} = \frac{1}{N+1}\left[\cos\left(\frac{N(k-j)\pi}{N+1}\right) - \cos\left(\frac{N(k+j)\pi}{N+1}\right)\right.$$
$$\left. + \sin\left(\frac{N(k-j)\pi}{N+1}\right)\frac{\cos((k-j)\pi/(N+1))}{\sin((k-j)\pi/(N+1))} - \sin\left(\frac{N(k+j)\pi}{N+1}\right)\frac{\cos((k+j)\pi/(N+1))}{\sin((k+j)\pi/(N+1))}\right]$$
$$(A.6)$$

In particular, if $k = j$ it follows that

$$\sum_{l=1}^{L}(M_1)_{lk}(M_1)_{lk} = \frac{1}{N+1}\left[1 - \cos(\frac{2kN\pi}{N+1}) + N - \sin(\frac{2kN\pi}{N+1})\frac{\cos(2k\pi/(N+1))}{\sin(2k\pi/(N+1))}\right]$$
$$= \frac{1}{N+1}\left[1 - \cos(\frac{2k\pi}{N+1}) + N + \sin(\frac{2k\pi}{N+1})\frac{\cos(2k\pi/(N+1))}{\sin(2k\pi/(N+1))}\right] = 1.$$

Similarly, if $k \neq j$ and again from (A.5), (A.6), we get

$$\sum_{l=1}^{L}(M_1)_{lk}(M_1)_{lj} = 0$$

thus establishing the orthogonality of M_1.

References

[1] R. Abgrall and J.-D. Benamou, Big ray tracing and eikonal solver on unstructured grids: Application to the computation of a multivalued traveltime field in the Marmousi model, Geophysics 64 (1999), 230–239.

[2] D. Andersh, J. Moore, S. Kosanovich, D. Kapp, R. Bhalla, R. Kipp, T. Courtney, A. Nolan, F. German, J. Cook, and J. Hughes, Xpatch 4: The next generation in high frequency electromagnetic modeling and simulation software, IEEE National Radar Conference – Proceedings, 2000, pp. 844–849.

[3] E. Bécache, P. Joly and C. Tsogka, Fictitious domains, mixed finite elements and perfectly matched layers for 2-D elastic wave propagation, J. Comput. Acoust. 9 (2001), 1175–1201.

[4] J.-D. Benamou, Direct computation of multivalued phase space solutions for Hamilton-Jacobi equations, Comm. Pure Appl. Math. 52 (1999), 1443–1475.

[5] E. Bleszynski, M. Bleszynski, and T. Jaroszewicz, AIM: Adaptive integral method for solving large-scale electromagnetic scattering and radiation problems, Radio Sci. 31 (1996), 1225–1251.

[6] B. Borden, Radar Imaging of Airborne Targets, Institute of Physics Publishing, Bristol, 1999.

[7] M. Born and E. Wolf, Principles of optics, Cambridge University Press, Cambridge, 1980.

[8] O. P. Bruno, C. A. Geuzaine, J. A. Monroe and F. Reitich, Prescribed error tolerances within fixed computational times for scattering problems of arbitrarily high frequency: the convex case, Phil. Trans. Roy. Soc. London 362 (2004) 629–645.

[9] O. Bruno and L. Kunyansky, A fast, high-order algorithm for the solution of surface scattering problems: basic implementation, tests and application, J. Comput. Phys. 169 (2001), 80–110.

[10] M.-H. Chen, B. Cockburn and F. Reitich, High-order RKDG methods for computational electromagnetics, J. Sci. Comput., to appear.

[11] L.-T. Cheng, M. Kang, S. Osher, H. Shim and Y.-H. Tsai, Reflection in a level set framework for geometric optics, CMES Comput. Meth. Sci. Eng. 5 (2004), 347–360.

[12] Jon F. Claerbout, Imaging the earth's interior, Blackwell Scientific Publications, Cambridge, MA, 1985.

[13] B. Cockburn and C.-W. Shu, The Runge-Kutta discontinuous Galerkin finite element method for conservation laws V: Multidimensional systems, J. Comput. Phys. 141 (1998), 199–224.

[14] B. Cockburn and C.-W. Shu, Runge-Kutta discontinuous Galerkin methods for convection-dominated problems, J. Sci. Comput. 16 (2001), 173–261.

[15] M. G. Crandall and P.-L. Lions, Viscosity solutions of Hamilton-Jacobi equations, Trans. Amer. Math. Soc. 277 (1983), 1–42.

[16] B. Engquist and O. Runborg, Computational high frequency wave propagation, Acta Numerica (2003), 181-266.

[17] B. Engquist, O. Runborg and A.-K. Tornberg, High-frequency wave propagation by the segment projection method, J. Comput. Phys. 178 (2002), 373–390.

[18] E. Fatemi, B. Engquist and S. J. Osher, Numerical solution of the high frequency asymptotic expansion for the scalar wave equation, J. Comput. Phys. 120 (1995), 145-155.

[19] S. Gottlieb, C.-W. Shu, and E. Tadmor, Strong stability preserving high order time discretization methods, SIAM Rev. 43 (2000), 89–112.

[20] J.S. Hesthaven and T. Warburton, Nodal high-order methods on unstructured grids. I. Time-domain solution of Maxwell's equations, J. Comput. Phys. 181 (2002), 186–221.

[21] G.-S. Jiang and D. Peng, Weighted ENO schemes for Hamilton-Jacobi equations, SIAM J. Sci. Comput. 21 (2000), 2126–2143.

[22] S. Operto, S. and Xu and G. Lambare, Can we image quantitatively complex models with rays?, Geophysics 65 (2000), 1223–1238.

[23] S. Osher, L.-T. Cheng, M. Kang, H. Shim and Y.-H. Tsai, Geometric optics in a phase-space-based level set and Eulerian framework, J. Comput. Phys. 179 (2002), 622–648.

[24] D. Peng, B. Merriman, S. Osher, H. Zhao, and M. Kang, A PDE-based fast local level set method, J. Comput. Phys. 155 (1999), 410–438.

[25] J. Qian, L.-T. Cheng and S.J. Osher, A level set based Eulerian approach for anisotropic wave propagations, Wave Motion 37 (2003), 365-379.

[26] J. Qian and S. Leung, A Level Set Method for Paraxial Multivalued Traveltimes, J. Comput. Phys. 197 (2004), 711-736.

[27] C. W. Shu and S. Osher, Efficient implementation of essentially nonoscillatory shock-capturing schemes, J. Comput. Phys. 77 (1988), 439–471.

[28] J.M. Song, C.-C. Lu, and W.C. Chew, Multilevel fast multiple algorithm for electromagnetic scattering by large complex objects, IEEE Trans. Antennas Propagat. 45 (1997), 1488–1493.

[29] R. J. Spiteri and S. J. Ruuth, A new class of optimal high-order strong-stability-preserving time discretization methods, SIAM J. Numer. Anal. 40 (2002), 469–491.

[30] M. Sussman and M. Y. Hussaini, A discontinuous spectral element method for the level set equation, J. Sci. Comput. 19 (2003), 479–500.

[31] W. W. Symes, A slowness matching finite difference method for traveltimes beyond transmission caustics, in Proceedings of 68th Annual International Meeting, Soc. Expl. Geophys., Expanded Abstracts, 1998, 1945–1948.

[32] W. W. Symes and J. Qian, A slowness matching Eulerian method for multivalued solutions of eikonal equations, J. Sci. Comp., 19 (2003), 501–526

[33] J. van Trier and W. W. Symes, Upwind finite-difference calculation of traveltimes, Geophysics 56 (1991), 812-821.

[34] J. Vidale, Finite-difference calculation of traveltimes, Bull. Seism. Soc. Amer. 78 (1988), 2062-2076.

[35] M. D. White and M. R. Visbal, Implicit high-order generalized coordinate solution of Maxwell's equations, Antennas and Propagation Society International Symposium, AP-S. Digest 3 (2002), 256–259.

[36] G. B. Whitham, Linear and Nonlinear Waves, Wiley, 1974.